Characterization of Feeder Effects on Continuous Solid Mixing Using Fourier Series Analysis

Yijie Gao, Fernando Muzzio, and Marianthi Ierapetritou
Dept. of Chemical and Biochemical Engineering, Rutgers—The State University of New Jersey, 98 Brett Road, Piscataway, NJ 08854

DOI 10.1002/aic.12348
Published online August 26, 2010 in Wiley Online Library (wileyonlinelibrary.com).

Variance reduction ratio (VRR) is generally considered as an important index in characterizing the continuous powder mixing. Although the capacity of the mixer to smooth out feeder fluctuations can be expressed by the VRR, few studies are performed quantitatively in this area. The feeder effects are investigated on the solid mixer through the Fourier series analysis. The VRR is deduced quantitatively using the Fourier series of the feed rate variability and the residence time distribution (RTD), which facilitate the explicit decomposition of VRR into intensities of different frequency components. It provides a novel model to determine whether the integrated feeder-mixer system satisfies specific solid mixing performance criteria, and provides guidelines of system improvement. © 2010 American Institute of Chemical Engineers *AIChE J,* 57: 1144–1153, 2011

Keywords: continuous mixing, Fourier series, variance reduction ratio

Introduction

Powder mixing is a widely used process in the manufacture of catalysts, cement, food, metal parts, and many other industrial products. In the pharmaceutical processing, a homogenized powder mixture is required to produce tablets with minimum variability, which is critical to meet strict regulatory constraints. This goal is usually realized using batch mixing, which is an easily implemented process in which two or more initially segregated materials are mixed, typically in a tumbling blender. However, recent work has been reported in the literature[1] toward developing continuous powder mixing processes that show enhanced productivity under integrated online controls.

The role of continuous mixing is to reduce segregation of fluxes that are fed continuously into the system. This process includes two parts[2]: first, two or more initially segregated components mix locally in the radial directions, which is similar to batch mixing. Second, axial mixing smoothes out feed rate fluctuations so that the requirement of uniform flowing streams can be met.[3] Focusing on the second part, earlier studies of continuous mixers involved the definition of variance reduction ratio (VRR), which was first introduced[4,5] as the ratio of variances for the input and output material flow rates in fluid continuous mixing systems. The case of perfect gas mixing was analyzed in a model of a single continuous stirred tank,[6] where feed rates with regular periodic fluctuations and completely random fluctuations were investigated. In solid mixing, batch to batch variability reduction was researched on semi-continuous blenders.[7] A predictive formula for variability of the output flow was then tested on free flowing nonsegregating powders,[8,9] where the sampling size was large enough to shield the contribution of local segregation to the experimental output variance. Extension of this formula was also investigated in continuous mixing of segregating powders[10] in a fluidized bed, where the variance component of powder segregation was first considered in the prediction of experimental output variance.

This article is dedicated to the memory of Professor Bruce Naumann, who did more than anyone else to make residence time distributions useful and understandable for two generations of chemical engineers.

Correspondence concerning this article should be addressed to M. Ierapetritou at marianth@soemail.rutgers.edu.

An alternative approach to describe the continuous mixing performance is to use the RTD (or derivative indices). Details of the RTD theory can be found in its 100th anniversary review.[11] Several predictive models have been developed to describe its nonidealities. For instance, a "delay and dead volume" model linked a PFR and a CSTR in the RTD simulation in a rotating drum, a single-screw extrusion process and a twin-screw continuous mixer;[9,12,13] a dispersion model based on the Fokker-Planck equation was detailed analyzed in different solid mixing processes;[14–17] Markov chains[1,18] and compartment models[19] were applied using networks of interconnected cells based on the flow structure of powder mixers. Based on the RTD theory and the previous studies of VRR, a comprehensive formula of VRR was proposed to summarize the two parts of the continuous mixing process.[20] In this formula, the variance of the output mixture consists of the remaining variability that the mixer fails to eliminate in both the axial and radial directions.

Although the VRR is widely used, several previous studies indicate its inaccuracy. Periodic feed fluctuations at different frequency lead to different VRR in the same mixer, indicating that VRR value at a single frequency of fluctuation is not sufficient to thoroughly capture the efficiency of the continuous mixer on smoothing input fluctuations. Furthermore, it is difficult to understand the contributions from either RTD or feed rate fluctuations on the value of the VRR. Little work has been done on quantifying the ability of the system to filter feed rate fluctuations,[2] and the relationship between the RTD profile and the filtering ability of the mixer is not clarified.

It has been reported that the VRR is dramatically amplified when the input fluctuation is at a higher frequency.[20] Moreover, a broader RTD curve results from larger axial dispersion, indicating better mixing performance, which is equivalent to a narrower low-pass filter.[2] In order to define this filtering ability of the mixer to mitigate input noise as a function of frequency, Fourier series analysis is introduced into this work.

Fourier series is a widely used mathematical tool in the applied sciences and has been applied in the field of solid mixing before. The applicability of discrete Fourier transform (DFT) has been tested on characterizing random and ordered solids mixtures.[21] It has also been employed on the autocorrelation function to determine the scale and intensity of time-dependent segregation.[20] In this work, we develop a general analytical method to characterize the feeder effects on continuous power mixing processes based on the definition of the VRR and the theory of Fourier series. The remainder of the article is organized as follows. In the next section, the methodology for practical estimation of the filtering ability of the mixer is presented. The spectrum of fluctuation variance distribution and the filtering ability are defined and derived. A case study of a real feeder-mixer system was then explored to practically illustrate the application of the method. A dispersion model was used to determine the RTD, and the results were applied to the VRR analysis. Then the article concludes with a summary and discussion.

Methodology

Introduction of the variance reduction ratio (VRR)

The earliest formula of the VRR[5] was derived to characterize the fluctuations of continuous fluid mixer

$$\frac{1}{VRR_{fluid}} = \frac{\sigma_{out}^2}{\sigma_{\text{in}}^2} = 2\int_0^\infty \int R(r)E(\theta)E(\theta+r)d\theta dr \quad (1)$$

$$R(r) = \frac{\overline{\delta_{\text{in}}(t)\delta_{\text{in}}(t-r)}}{\sigma_{\text{in}}^2} \quad (2)$$

$$C_{\text{in}}(t) = \overline{C_{\text{in}}} + \delta_{\text{in}}(t) \quad (3)$$

where $R(r)$ in Eq. 2 describes the autocorrelation coefficient or serial correlation coefficient. $C_{\text{in}}(t)$, expressed as sum of the mean value $\overline{C_{\text{in}}}$, and the fluctuation part $\delta_{\text{in}}(t)$ in Eq. 3, is denoted as input feed rate. $E(t)$, defined as the normalized residence-time distribution (RTD), is derived from the measured residence-time distribution $C(t)$ using Eq. 4

$$E(t) = \frac{C(t)}{\int_0^\infty C(t)dt} \quad (4)$$

As mentioned earlier, Eq. (1) was designed for fluid mixing. A modification suitable for solid mixing characterization was suggested based on the limited homogeneity of output mixture[20]

$$\frac{1}{VRR_{\text{solids}}} = \frac{1}{VRR_{\text{fluid}}} + \frac{\sigma_{\text{out, idealfeed}}^2}{\sigma_{\text{in}}^2} \quad (5)$$

In Eq. 5 VRR_{solids} expresses the overall VRR of solid continuous mixing. The fluid mixing part VRR_{fluids} indicates the variance from the remainder of feed rate fluctuations that the mixer fails to smooth out. The solid mixing part $\sigma_{\text{out,idealfeed}}^2/\sigma_{\text{in}}^2$, can be represented by the value of VRR under ideal feed rate conditions. In this study, since we focus on the contribution of feeder fluctuations to the output variance, the ideal feed part is not considered in the following sections. Several assumptions necessary for the following Fourier analysis on the fluid mixing formula of VRR are discussed in the next subsection.

Assumptions for the Fourier series application

The standard form of Fourier series is as follows

$$f(x) = \frac{a_0}{2} + \sum_{n=1}^{\infty}[a_n\cos(nx) + b_n\sin(nx)], \quad x \in [-\pi, \pi] \quad (6)$$

$$a_n = \frac{1}{\pi}\int_{-\pi}^{\pi} f(x)\cos(nx)dx;\ b_n = \frac{1}{\pi}\int_{-\pi}^{\pi} f(x)\sin(nx)dx \quad (7)$$

where $f(x)$ is a real variable function with period 2π on the interval $[-\pi, \pi]$; a_n, b_n are the coefficients of the n^{th} frequency component of the sine and cosine function series. Using Eq. 6, the variance of the function can be expressed as the sum of squares of a_n and b_n, due to the orthogonal relationships of the sine and cosine functions

$$\sigma^2 = \frac{\int_{-\pi}^{\pi}(f(x) - \overline{f(x)})^2 dx}{2\pi} = \sum_{n=1}^{\infty}\frac{a_n^2 + b_n^2}{2} = \sum_{n=1}^{\infty}\frac{s_n^2}{2} \quad (8)$$

In Eq. 8, the frequency component of the variance of $f(x)$ is expressed as half of the corresponding square of frequency

intensity $s_n^2 = a_n^2 + b_n^2$. One of the major advantages of Eq. 8 is that it can illustrate the frequency distribution of the feeding fluctuations. In order to apply this analysis into continuous mixing processes, three assumptions are required as follows.

First, the function of residence time distribution $E(\theta)$ is assumed to be time-invariant in the mixing process. This assumption is valid in most cases since residence time distribution is the probability distribution of a large number of particles in the pulse test. In other words, we assume that the fluctuations in composition at the entrance of the mixer do not significantly alter the flow of the powder through the mixer. It is based on the application of RTD in Danckwerts' formula.[5]

$$C_{\text{out}}(t) = \int_0^\infty C_{\text{in}}(t-\theta)E(\theta)d\theta \tag{9}$$

Due to the definition of Fourier series, the periodic function $f(x)$ in Eq. 6 is defined on the interval $[-\pi, \pi]$; however, the definition domains for both $C_{\text{in}}(t)$ and $E(\theta)$ in Eq. 9 are from zero to infinity, while both feed rate fluctuations and RTD can only be recorded for finite times in practice. Due to these limitations, another assumption is that the magnitude of $E(\theta)$ is negligible at the end of the RTD measurement. This makes sure that the recorded $C_{\text{in}}(t)$ and $E(\theta)$ can be truncated and transformed onto the interval $[-\pi, \pi]$ without missing significant signal information. Exception to this assumption could occur when the mixer has quasi-stagnant regions exchanging mass very slowly with the main flow. Solution of this issue is discussed later.

The last assumption concerns the Dirichlet conditions which describes the sufficient condition that guarantees that the Fourier series convergence. Based on the Dirichlet conditions the sufficient conditions for the Fourier series to converge is that the function $f(x)$ should be bounded, absolutely integrable, and have a finite number of discontinuities and extrema in any given interval. The conditions should be satisfied for $C_{\text{in}}(t)$ and $C_{\text{out}}(t)$ so that the reconstructed functions based on their Fourier series are equal to the original functions at each point where $C_{\text{in}}(t)$ and $C_{\text{out}}(t)$ are continuous.

Application of Fourier series analysis

Based on Eqs. 6 and 7, and the assumptions in the last subsection, the continuous functions of feed rate fluctuations $C_{\text{in}}(t)$, and the residence time distribution $E(t)$ in Eq. 9 were transformed onto the interval $[-\pi, \pi]$, and substituted by the corresponding Fourier series. The final output variance and VRR formula of Fourier series are as follow

$$\sigma_{\text{out}}^2 = \pi^2 \sum_{n=1}^{\infty} \frac{(a_n^2 + b_n^2)(A_n^2 + B_n^2)}{2} = \sum_{n=1}^{\infty} \frac{s_n^2 F_n^2 \pi^2}{2} \tag{10}$$

$$\frac{1}{VRR} = \frac{\sigma_{\text{out}}^2}{\sigma_{\text{in}}^2} = \frac{\sum_{n=1}^{\infty}(a_n^2 + b_n^2)(A_n^2 + B_n^2)\pi^2}{\sum_{n=1}^{\infty}(a_n^2 + b_n^2)} = \frac{\sum_{n=1}^{\infty} s_n^2 F_n^2 \pi^2}{\sum_{n=1}^{\infty} s_n^2} \tag{11}$$

where a_n, b_n, are the Fourier series coefficients of the transformed feed rate $f_{\text{in}}(t)$ at the n^{th} frequency component, and the square of the frequency intensity is denoted as $s_n^2 = a_n^2 + b_n^2$; similarly A_n, B_n and $F_n^2 = A_n^2 + B_n^2$ are the Fourier series coefficients and the square of frequency intensity of the transformed RTD function $e(x)$. Detailed derivation can be found in the Appendix. Due to the expression of VRR in Eq. 11, the filtering ability of the mixer is frequency dependent, expressed by the term $F_n^2\ \pi^2$. Notice that this filtering ability should not be larger than one since amplification of signal fluctuations is impossible in the continuous mixing process. Comparison between Eqs. 1 and 11 indicates that the new VRR formula can clearly illustrate the contributions of either feed rate fluctuations or RTD profiles to the output variance of the system, in different frequency domains.

In order to utilize this new VRR formula in practice, we need to introduce the discrete Fourier transform, as continuous records of feed rate and RTD signals with infinite sampling frequency are not available. Moreover, since the scale of the Fourier coefficients is discrete on the frequency domain, and thus is proportional to the sample length, it is difficult to compare variance distributions from feeding samples with different length. To solve these problems, procedures are described as follows.

The expressions of discrete Fourier series are shown in Eqs. 12 and 13, where N is the number of signal points evenly sampled, and x_n is the measured value of each point and X_n is the Fourier component of the k^{th} frequency

$$X_k = a_k + ib_k = \frac{2}{N}\sum_{n=0}^{N-1} x_n e^{-\frac{2\pi i}{N}kn}, \quad k = 1, 2, \ldots N-1 \tag{12}$$

$$a_k = \frac{2}{N}\sum_{n=0}^{N-1} x_n \cos\frac{2\pi}{N}kn; \quad b_k = -\frac{2}{N}\sum_{n=0}^{N-1} x_n \sin\frac{2\pi}{N}kn \tag{13}$$

$$\sigma^2 = \sum_{n=1}^{N/2} \frac{s_n^2}{2} \tag{14}$$

In Eq. 14, the term s_n^2 has the same definition as that of the continuous form in Appendix. By comparing Eqs. 12 and 13 with the corresponding ones for the continuous case (6) and (7), respectively, it is found that N is expressed as $N = T_{\text{in}}/\Delta t$. Here T_{in} denotes the length of feed rate sample, and Δt is the sampling interval, which is the reciprocal of the sampling frequency.

One of the common problems caused by the discrete method of data collection is what is called aliasing in the field of signal analysis, which describes the inaccuracy of fluctuation signal measurement around the sampling frequency (Figure 1). To eliminate measurement error caused by aliasing, the maximum frequency component we use in Fourier series is half of the sampling frequency. For example, if the sampling time interval is 0.1 s, the sampling frequency is 10 Hz, and the maximum frequency we should use in Fourier series calculation is 5 Hz. Thus, all the frequency components between $n \in [N/2 + 1, N - 1]$ are higher than half of the sampling frequency, and are dropped off in the variance calculation in Eq.14.

Due to Eq. A7 in the Appendix, the sum of squares of all the coefficients a_k and b_k in Eq. 13 is constant for the same feed rate sample. It indicates that the magnitude of these coefficients is reciprocally proportional to the number of sampling points N, or to the sampling interval Δt when feed rate samples are in the same length. Continuous integration formula instead of sum of squares is, thus, necessary to avoid the inconsistence caused by different Δt, using Eqs. 14 and 15.

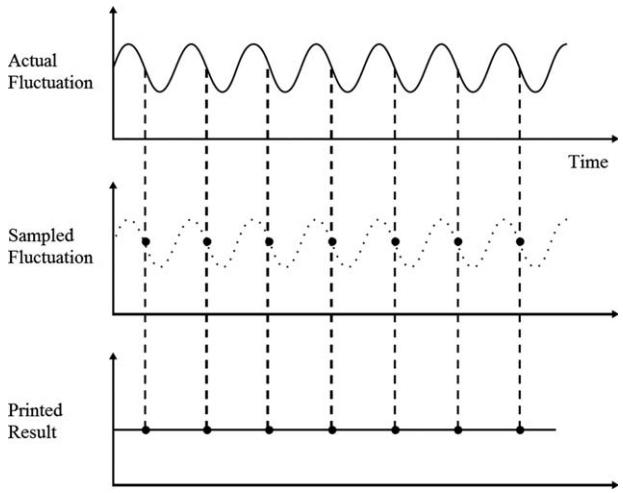

Figure 1. Signal fluctuation intensity at sampling frequency may be distorted because of aliasing.

When aliasing occurs, the signal intensity is possibly masked or mistakenly combined to that of a lower frequency. To avoid this problem, the common method is to abandon the signal intensity on the range between half and a whole sampling frequency.

$$\sigma^2 = \frac{1}{2}\int_0^{f_{\max}/2} s(f)^2 df \approx \sum_{n=1}^{N/2} \frac{s(n\Delta f)^2}{2}\Delta f \tag{15}$$

$$s(n\Delta f) = \frac{s_n}{\sqrt{\Delta f}} \tag{16}$$

In Eq. 16, we introduce the continuous form *s(f)* instead of the discrete variance component series s_n. Here $\Delta f = 1/T_{\text{in}}$ is the minimal frequency interval in the Fourier series, and $f_{\max}/2$ denotes half of the frequency of sampling, corresponding to the $N/2$ component of the variance intensity. Equation 16 represents the continuous variance intensity distribution derived from the discrete series, and the scale of this distribution is independent of how long the feed rate sample is recorded, or how many points are sampled on the signal of feed rate.

Comparing Eqs. 15 and 16 with the continuous formula of output variance, or VRR in Eqs. 10 and 11, we define the ability of a continuous mixer to filter out feed rate fluctuations as $Fe(f)$

$$Fe(f) = F(f)\pi \tag{17}$$

where $F(n\Delta f) = F_n$ indicates that the magnitude of filtering ability is independent of the number of sampling points. It should be noticed that the coefficient π in Eq. 17 comes from the conversion of time scale from $t \in [0, T_{\text{in}}]$ to $x \in [-\pi, \pi]$. If this conversion step is not applied, Eq. 17 is replaced by a general form where $F(f)$ is now directly from the Fourier series of $E(t)$

$$Fe(f) = \frac{F(f)T_{\text{in}}}{2} \tag{18}$$

Substituting Eqs. 15–17 into Eqs. 10 and 11, we derive the applicable form of output variance and VRR

$$\sigma_{\text{out}}^2 = \frac{1}{2}\int_0^{f_{\max}/2} s(f)^2 Fe(f)^2 df \tag{19}$$

$$\frac{1}{VRR} = \frac{\sigma_{\text{out}}^2}{\sigma_{\text{in}}^2} = \frac{\int_0^{f_{\max}/2} s(f)^2 Fe(f)^2 df}{\int_0^{f_{\max}/2} s(f)^2 df} \tag{20}$$

where $s(f)$ is the variance spectrum, and $Fe(f)$ is the filtering ability of the mixer. It becomes clear that for the input variance component $s(f)^2\Delta f/2$ at a small frequency range $[f - \Delta f/2, f + \Delta f/2]$, a fraction of $1 - Fe(f)^2$ of that variance component will be filtered out by the mixer. This formula shows its merit in clarifying the criterion for design and selection of a mixer or a feeder in an integrated system. Examples of analysis of $Fe(f)$ with different parameters and applications of Eqs. 19 and 20 will be discussed in detail later.

Correction of the RTD in Fourier series analysis

In *Methodology* we assumed that RTD is negligible on $t \in (T_{\text{in}}, \infty)$, which guarantees the validity of Eq. A8 in the Appendix. However, this is not the case when the tail of $E(t)$ is still significant around the time point $t = T_{\text{in}}$. For instance, $E(2\tau)$ equals 0.1353 in the case of one-tank CSTR. If we select $T_{\text{in}} = 2\tau$ as the length of feed rate sample, the application of the previous analysis to this RTD will introduce error due to the truncation of the significant RTD tail. The original assumption of negligible RTD tail should be improved to eliminate this problem.

The solution for this problem can be found on the characteristics of the extended periodical function of the Fourier series. Because the feed rate fluctuation sample is assumed to be a periodic function that is extended infinitely (dash line in Figure 2a), the output fluctuation is also a periodic function due to Eq. 9

$$C_{\text{in}}(t) = C_{\text{in}}(t + iT_{\text{in}}), \quad i \in Z \tag{21}$$

$$C_{\text{out}}(t) = \int_0^{\infty} C_{\text{in}}(t + iT_{\text{in}} - \theta)E(\theta)d\theta = C_{out}(t + iT_{\text{in}}), \quad i \in Z \tag{22}$$

Here the period of the extended functions $C_{\text{in}}(t)$ and $C_{\text{out}}(t)$ equals the feed rate sample length T_{in}. Using Eqs. 21 and 22, an equivalent RTD $E'(t)$ that is negligible on the domain $t \in (T_{in}, \infty)$ is created, which leads to the same output periodic function as that of the original RTD function

$$E'(t) = \begin{cases} \sum_{i=0}^{\infty} E(t + iT_{\text{in}}), & t \in [0, T_{\text{in}}] \\ 0, & t \in (T_{\text{in}}, \infty) \end{cases} \tag{23}$$

$$\int_0^{\infty} C_{\text{in}}(t-\theta)E(\theta)d\theta = \sum_{i=0}^{\infty}\int_0^{T_{\text{in}}} C_{\text{in}}(t-\theta-iT_{\text{in}})E(\theta+iT_{\text{in}})d\theta = \int_0^{T_{\text{in}}} C_{\text{in}}(t-\theta)E'(\theta)d\theta \tag{24}$$

The correction of RTD illustrated in Eqs. 23 and 24 makes it possible to apply the Fourier series even if the assumption of

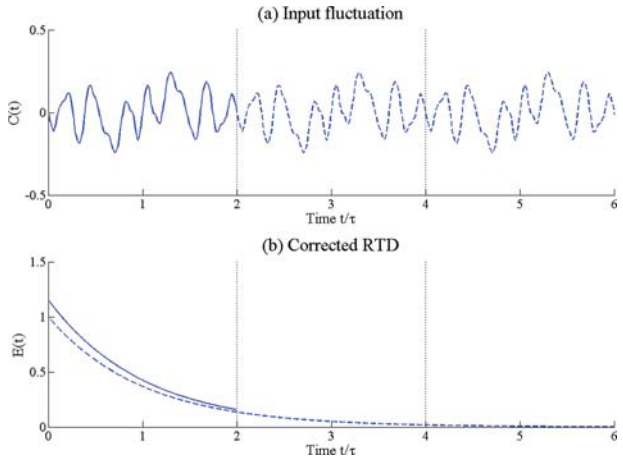

Figure 2. The correction of the RTD can be derived by the characteristics of extended periodical function in the Fourier series.

The length of the feed rate sample in (a) is 2τ. However, $E(t)$ is not completely ignorable after that time point $t = 2\tau$, so the assumption of the negligible RTD on the domain $t \in (T_{in}, \infty)$ is not satisfied here. To solve this problem, the time period 2τ is used as one time unit to form the corrected RTD (b) (solid line), which is created by the superposition of the original RTD (dash line) from different time units. The corrected RTD will produce the same output as the original one without loss of information. [Color figure can be viewed in the online issue, which is available at wileyonlinelibrary.com.]

negligible RTD on the domain $t \in (T_{in}, \infty)$ is not satisfied (Figure 2). This analysis will be used in the case study in the following section.

Case study: a real feeder-mixer combination

In this section, the developed methodology is applied using data obtained from a continuous feeder-mixer integrated system. Feed rate data $C_{in}(t)$ of excipient (lactose) and active pharmaceutical ingredient or API, as well as experimental residence time distribution, are collected.

A GCM 250® convective continuous mixer is used in this case study, which is operated at a blade speed of 250RPM with all blade angles 20° forward. Two loss-in-weight (LIW) feeders provided by Schenck-Accurate are used to feed the mixer. Acetaminophen (with average particle size of 45 μm), preblended with 0.25% SiO_2, is used as a representative active pharmaceutical ingredient (API), and microcrystalline cellulose (Avicel PH200, 240 μm) is used as the main excipient.

In the continuous mixing process, the mass fraction of API in this case study is set as 3%, and the overall mass feed rate is 66.2 kg/h. The feed rate variability of API and excipient are separately measured at the corresponding feed rates, using a catch-scale that records the weight of powder discharged by the feeder as a function of time. More specifically, a container is placed on the catch scale and powder is fed for about 30 min. With a sampling frequency of 10 Hz, the temporal feed rates $C_{in}(t)$ of both components are calculated based on the weight increase in the container. Several feed rate samples of 100 s are then randomly selected from the 30 min record. The continuous variance spectrums $s(f)$ of these samples are calculated. Since no significant difference is observed between these spectrums, a feed rate sample of 100 s is long enough to represent the variability characteristics for both components, and the feed rate sample measured by the catch-scale is eligible to represent the feed rate fluctuations in real continuous mixing process.

In the corresponding RTD measurement, 10 g API is used as the pulse. The feed rate of excipient is equal to the sum of feed rates of the exicipent and the API in the continuous mixing process. After the pulse is injected at the input, samples are manually collected at the output of the mixer at a sampling frequency of 0.25 Hz. The disturbance to the bulk flow caused by the injection of the tracer is assumed to be negligible. As samples are collected, they are analyzed by NIR spectroscopy to determine the concentration of acetaminophen ($C(t)$). The residence-time distribution ($E(t)$) is then calculated based on the collected concentration data and Eq. 4. To exclude the influence of irregular fluctuations, a curve fitting process is applied on raw RTD data using the Taylor dispersion model, described as follows.

Taylor dispersion model

The mixing efficiency of RTD is most commonly characterized by its dimensionless second moment of the mean residence time[11]

$$\sigma_{2nd}^2 = \frac{\int_0^\infty (t-\tau)^2 E(t)dt}{\tau^2} \tag{25}$$

where the subscript $2nd$ is used to distinguish this metric from the variance discussed in the previous sections. It has been reported that in PFR $\sigma_{2nd}^2 = 0$ and in CSTR $\sigma_{2nd}^2 = 1$, but little regarding the mixing efficiency has been discussed when the value of σ_{2nd}^2 is between zero and one. In this subsection, the filtering ability index developed in this work is used to characterize the influence of parameters to the filtering ability of the Taylor dispersion model

$$\frac{\partial C}{\partial \theta} + \frac{\partial C}{\partial \xi} = \frac{1}{Pe}\frac{\partial^2 C}{\partial \xi^2} \tag{26}$$

$$C(\xi,\theta) = \frac{C_0 Pe^{1/2}}{(4\pi\theta)^{1/2}} e^{\frac{-Pe(\xi-\theta)^2}{4\theta}} \tag{27}$$

Equation 26 illustrates the Fokker-Planck equation.[22] A simplified solution, shown in Eq. 27, is the Taylor dispersion model, where $\theta = t/\tau$ and $\xi = z/l$ are the dimensionless time and location, and Pe is the Peclet number, which serves in characterizing the dispersion of the flow system

$$Pe = vl/E \tag{28}$$

v and E are the axial velocity and dispersion coefficient of the system elements. At the outlet of the continuous mixer the concentration $C(\xi = 1, \theta)$ is only a function of θ, which can be normalized to deduce residence-time distribution with only one parameter Pe. The filtering ability $Fe(f)$ of the RTD modeled by Taylor dispersion model are plotted in Figure 3, with different. The plot indicates that better filtering ability of the mixer occurs for smaller Pe due to lower and narrower $Fe(f)$ curve. On the other hand, the model acts more like a PFR when Pe is large, in which no smoothing takes place in the

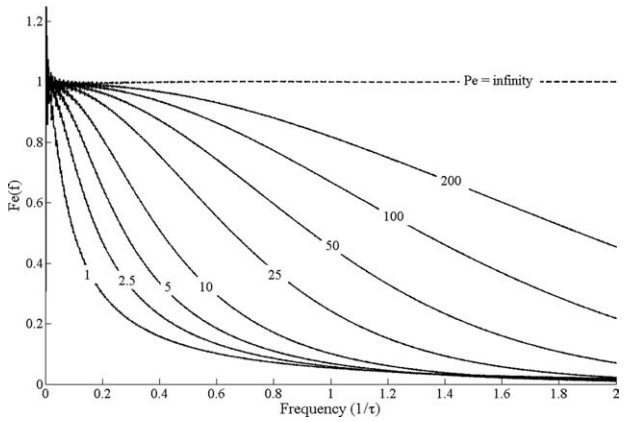

Figure 3. Filtering ability *Fe(f)* of the Taylor Dispersion model with different Peclet numbers from one to infinite.

The maximum value of Fe (f) is unity in the case of PFR.

mixer. $Fe(f)$ equals one for all frequency components in PFR, while all other curve profiles with finite Peclet numbers are below it. Figure 3 indicates the advantage of the proposed method when compared with the form σ^2_{2nd}.

The parameters Pe and τ in the dispersion model are optimized so that the mean sum of square of the residuals between the fitted curve and experimental data is minimized

$$\min MSS = \min \sum_{i=1}^{n} \frac{[C_i - C(t_i, Pe, \tau)]^2}{n} \tag{29}$$

where n is the number of measurement points in one RTD test, and t_i, C_i and $C(t_i, Pe, \tau)$ represent the time, experimental concentration and the fitted concentration of the i^{th} point, respectively. The fitted curve represented by the optimized set of parameters is used in the developed method.

Case study on continuous mixing data

In this case study, $E(t)$ and $C_{in}(t)$ obtained in continuous mixing experiments are converted to the filtering ability $Fe(f)$ and the continuous variance spectrum $s(f)$ for both excipient and API, which can be directly analyzed to clarify the performance of the system, and, thus, provide some guidelines for improvement.

In Figure 4a the fitted RTD function $E(t)$ is characterized by the optimized parameters $Pe = 1.76$ and $\tau = 3.66$ s. The filtering ability profile is computed and shown in Figure 4d using Eqs. 9, 12, and 27. It is observed that the fluctuations at frequencies higher than 0.25 Hz are almost completely filtered out, while below 0.1 Hz the mixer is not so efficient at filtering out fluctuations. In Figure 4b and c, dashed lines represent the feed rate samples $C_{in}(t)$ of excipient (denoted as EPT in the figure) and API. The length of of the samples are 100 s, as described earlier. By applying Eq. 9, the

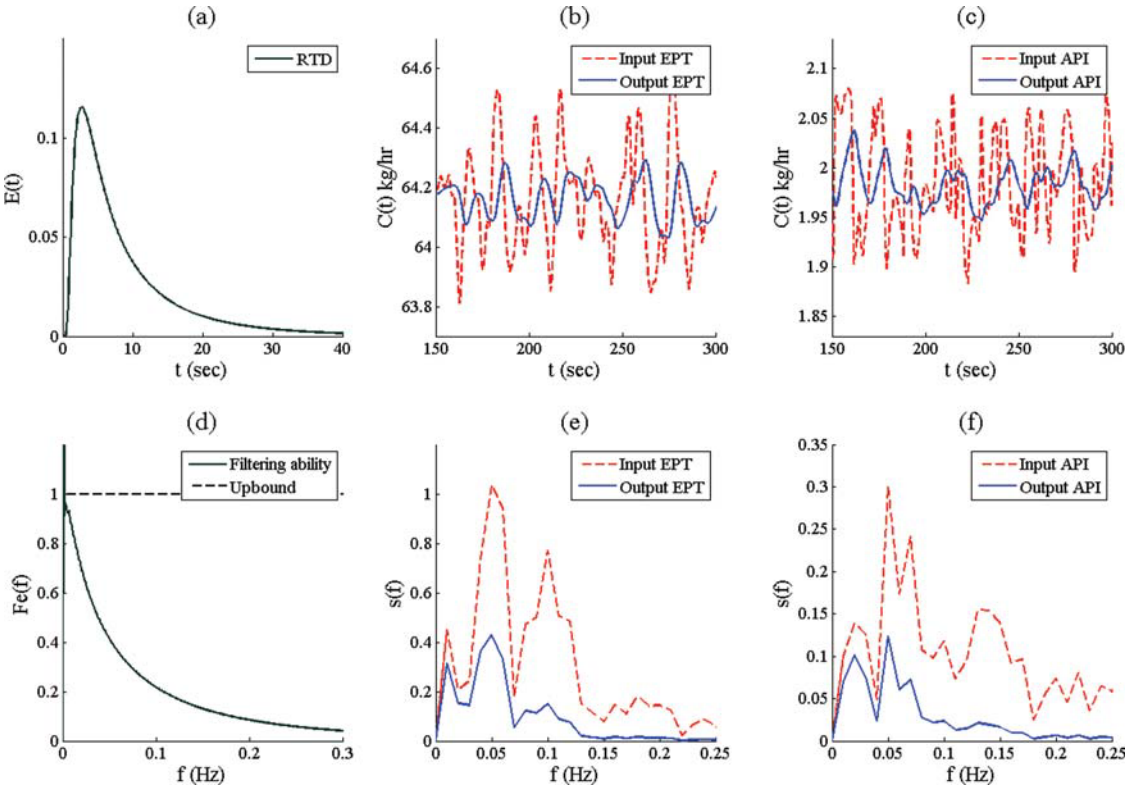

Figure 4. Summary of the case study.

(a) Fitted RTD curve, representing the mixer performance in the operation conditions of flow rate 66.2 kg/h, blade angle 20° forward, and rotary speed 250 RPM, (b) mass flow rate fluctuation of the excipient (EPT) at input and output streams, (c) mass flow rate of the API, (d) filtering ability $Fe(f)$ of the fitted RTD curve, (e) continuous variance spectrum $s(f)$ of the excipient, and (f) continuous variance spectrum of the API. [Color figure can be viewed in the online issue, which is available at wileyonlinelibrary.com.]

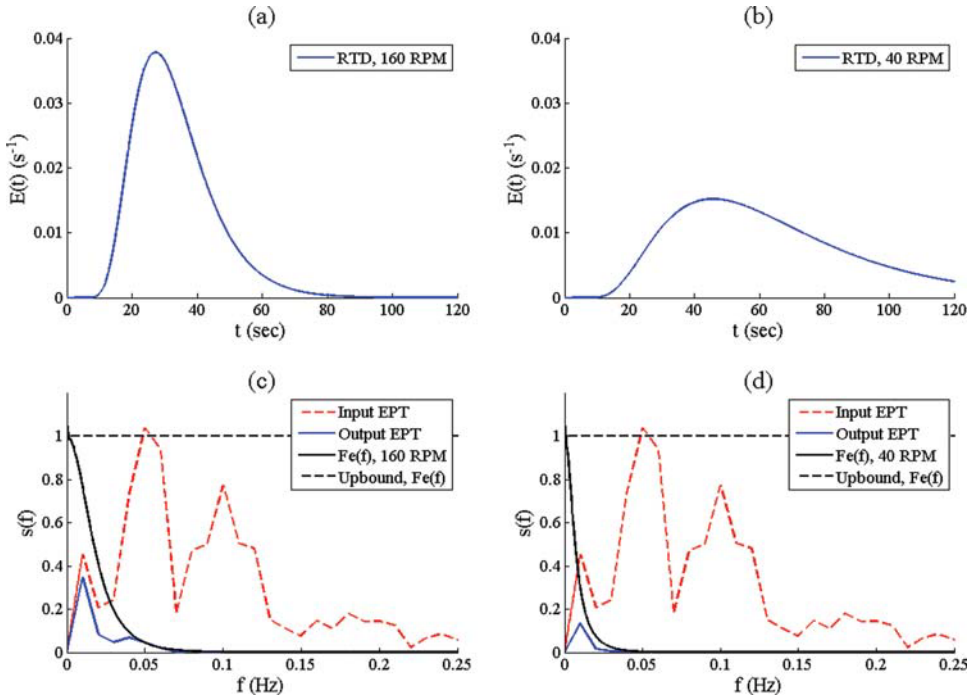

Figure 5. Filtering process using alternative RTDs.

(a) Fitted RTD curve at 160 RPM, (b) fitted RTD curve at 40 RPM, (c) filtering of variance spectrum by the RTD at 160 RPM, and (d) filtering of variance spectrum by the RTD at 40 RPM. The excipient feed rate sample in Figure 4 is used. [Color figure can be viewed in the online issue, which is available at wileyonlinelibrary.com.]

fluctuation of the output mass flow rate $C_{out}(t)$ can be calculated (Figure 4b and c, solid lines). Notice that since the feed rate samples $C_{in}(t)$ are not real-time feed rates in conitnuous mixing experiments, the calculated $C_{out}(t)$ are estimations of the output flow rates. Complete validation of the prediction of $C_{out}(t)$ can be performed when measurements of input and output flow rates are available.

Based on the feed rate samples and output flow rate predictions, a detailed variance reduction profile is illustrated in the continous variance spectum $s(f)$ in Figure 4e and f. It can be observed that the output varince component is negligible at frequency larger than 0.25 Hz in this case study. For both excipient and API, peaks of fluctuations are significant at 0.05 Hz in the input feed rate, while as much as 40% of the peaks survive through the mixing process. In this perspective, the system is not in its optimal set. Based on the profile of $s(f)$ and $Fe(f)$, either shifting the peaks of feeder fluctuations to a frequency higher than 0.25 Hz, or increasing the filtering ability below 0.1 Hz or both improve the efficiency of the system. For instance, the attenuation of the same excipient feed rate sample by alternative RTDs, measured at 160 RPM and 40 RPM rotary speeds, are shown in Figure 5. The fitting parameters are $Pe = 14.77$, $\tau = 29.17$ s, and $Pe = 7.40$, $\tau = 52.17$ s, respectively. Compared with the 250 RPM case in Figure 4, it can be seen that better filtering is achieved at the lower rotary speeds. The variance peak of the feed rate sample at 0.05 Hz is almost completely attenuated due to the small values of $Fe(f)$ at that frequency.

Applying Eqs. 19 and 20, the input and output variances, as well as the VRR can be calculated based on the integration of variance spectrums in Figure 4e and f, using the proposed frequency domain method. These values can also be calculated based on the time domain method using Eqs. 1 and 8. As shown in the results (Table 1) the two methods give consistent results indicating the convergence of the variance spectrum, which means that the assumption of Dirichlet conditions in *Methodology* is valid.

Preliminary design of a mixing system with an optimum RTD

Since the RTD is considered as an indicator of the mixer performance to some extent; many studies have been focused on characterizing the relationship between operating conditions and the shape of the RTD under these conditions. Several idealized categories of mixers such as PFR, CSTR, and the combination of these two basic elements are used to model the mixing of different cases.[12,18,23] However, few studies have reported on the quantitative design of RTD beyond these categories. Besides estimating existing continuous mixers, this study can also be used for the design of RTD with desired filtering ability.

Table 1. Validation of Case Study on the Experimental Data

Component		Frequency domain method	Time domain method
Excipient	σ_{in} (kg/hr)	.164	.164
	σ_{out} (kg/hr)	.067	.067
	VRR	6.01	6.02
API	σ_{in} (kg/hr)	.051	.051
	σ_{out} (kg/hr)	.023	.023
	VRR	4.91	4.91

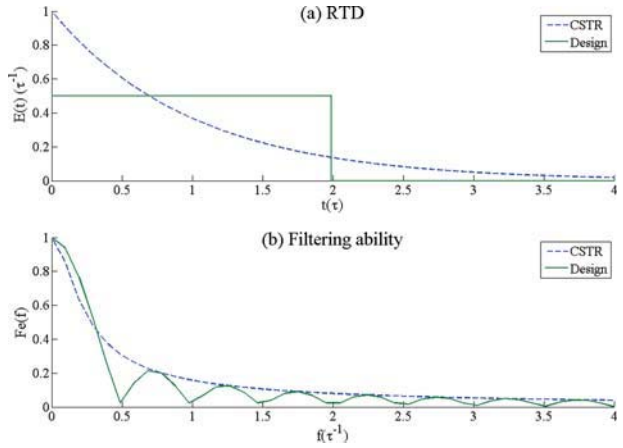

Figure 6. Comparison between CSTR and the designed RTD with the same mean residence time.

[Color figure can be viewed in the online issue, which is available at wileyonlinelibrary.com.]

The first constraint on RTD functional form is

$$\frac{A_0}{2} = \overline{e'(x)} = 1/2\pi \tag{30}$$

The average concentration $\overline{e'(x)}$ of RTD is predetermined due to the unity integration of the RTD $e'(x)$ on $x \in [-\pi, \pi]$. Notice that $e'(x)$ denotes the transformation of the corrected RTD defined before. The next constraint is $e'(x) \geq 0$ since probability distribution cannot be negative. Based on these two constraints, fluctuation at a single frequency can be considered in the RTD formula

$$e'(x) = \frac{1}{2\pi}(1 + b\cos kx) \tag{31}$$

$$Fe(f) = \begin{cases} |b|/2, & f = k/2\pi \\ 0, & f = i/2\pi \end{cases} \tag{32}$$

where $|b| \leq 1$, k, $i \in Z^+$ $(i \neq k)$ and $x \in [-\pi, \pi]$.

Equation 32 indicates that the RTD can filter out feeding fluctuations spaced at the interval $\Delta f = 1/2\pi$ except at $f = k/2\pi$. When $b = 0$, Eq. 31 regresses to a step function

$$e'(x) = \begin{cases} 1/2\pi, & x \in [-\pi, \pi] \\ 0, & x \notin [-\pi, \pi] \end{cases} \tag{33}$$

where fluctuations at $f = k/2\pi$ can also be depressed in this case. Thus, the corresponding original RTD is a step function with mean residence time τ, and width of 2τ. The step RTD function and its filtering ability calculated at $T_{in} = 50\tau$ are shown in Figure 6. The cases of cosine RTD functions with different values of b and k are also plotted (Figure 7), which indicate worse filtering abilities than the step function. When compared with the RTD of CSTR with the same mean residence time, the step RTD shows better filtering ability at the regions above half of the characteristic frequency, while at lower frequencies the CSTR can smooth out more fluctuations. Oscillation with the CSTR curve as the up bound occurs on the step RTD. Minima of the step RTD are found at equidistant frequencies, while maxima between each two of the minima coincide with points on the CSTR curve at corresponding frequencies. This suggests that although CSTR is considered as the most efficient back-flux mixing pattern that can be achieved in a continuous flowing systems, an RTD that is arbitrarily designed following the knowledge of the Fourier series may achieve much better mixing efficiency in some regions of fluctuation frequency. This provides another standard for the design of RTD instead of the CSTR.

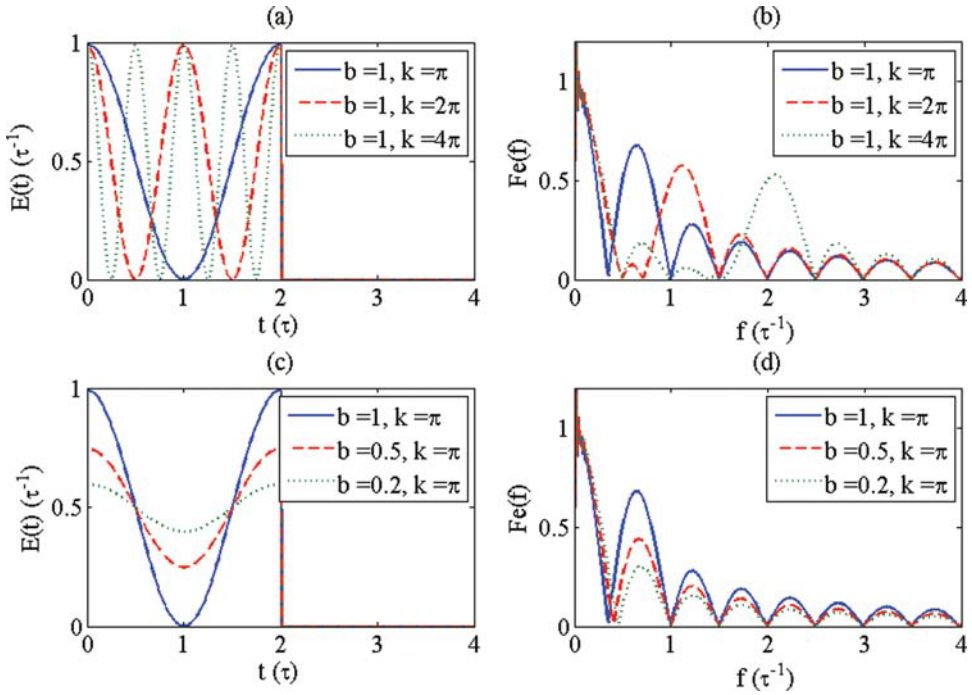

Figure 7. RTD and filtering ability of different *b* and *k* values.

[Color figure can be viewed in the online issue, which is available at wileyonlinelibrary.com.]

Based on the conception proposed by Zwietering,[23] the mixer with the step RTD can be conveniently constructed by modeling of a parallel array of plug-flow reactors with uniformly distributed length.

Summary and Conclusions

For many powder processes, continuous mixers provide a rarely used alternative to the widely used batch mixers. At this time, continuous mixing systems are of special interest in many industrial fields. Although the capacity of a continuous mixer to smooth out variability from feeders can be expressed by integrating the residence time distribution and the feed rate, little work has been published to clarify the filtering ability of the mixer when different feeders are involved. In this article, the variance reduction ratio was further analyzed by applying Fourier series methods. Input and output variance, as well as the filtering ability of the mixer, were decomposed into different frequency components. Based on the derivation in continuous flow function in the Appendix, the discrete form of the Fourier series was developed. The coefficients of the Fourier series transformation were also converted into continuous spectrum, which can be easily used to evaluate the system when different feeders and mixers were integrated.

The relationship between the filtering ability and the parameter of the Taylor dispersion model was also studied. In the dispersion model, increasing the Peclet number reduces the filtering ability significantly, and extremely large Peclet numbers convert the system into a PFR, where the mixer fails to smooth out any input variability. The derived conception of filtering ability can also be applied in characterizing other RTD models, where the influence of model parameters can clearly be estimated.

In this study, experimental feed rate and RTD data were used to test the applicability of this method. Based on the developed functions and, the efficiency of the feeder-mixer integration can be evaluated, and this provided crucial input for system improvement. Preliminary applications were also carried out on the design of residence-time distribution. A simple case of step function was generated, which even filtered out more fluctuations than CSTR in the designed frequency domains. Since the feeder fluctuations that cannot be filtered out are an essential contribution to the overall output variance of the feeder-mixer system, this work provided a novel approach for improving the design and quality control of continuous mixing system for industrial manufacturing.

Acknowledgments

The authors would like to thank the National Science Foundation for their financial support through grants NSF-0504497 and NSF-ECC 0540855.

Literature Cited

1. Marikh K, Berthiaux H, Mizonov V, Barantseva E, Ponomarev D. Flow analysis and markov chain modelling to quantify the agitation effect in a continuous powder mixer. *Chem Eng Res Des*. 2006; 84(11):1059–1074.
2. Pernenkil L, Cooney CL. A review on the continuous blending of powders. *Chem Eng Sci*. 2006;61(2):720–742.
3. Williams JC. Continuous mixing of solids. A review. *Powder Technol*. 1976;15(2):237–243.
4. Beaudry JP. Blender efficiency. *Chem Eng*. 1948;55:112–113.
5. Danckwerts PV. Continuous flow systems: Distribution of residence times. *Chem Eng Sci*. 1953;2(1):1–13.
6. Danckwerts PV, Sellers SM. The effect of holdup and mixing on a stream of fluctuating composition. *Ind Chem*. 1951;27:395.
7. Goldsmith PL. The theoretical performance of a semi-continuous blending system. *Statistician*. 1966;16(3):227–251.
8. Williams JC, Rahman MA. Prediction of the performance of continuous mixers for particulate solids using residence time distributions Part I. Theoretical. *Powder Technol*. 1972;5(2):87–92.
9. Williams JC, Rahman MA. Prediction of the performance of continuous mixers for particulate solids using residence time distributions: Part II. Experimental. *Powder Technol*. 1972;5(5):307–316.
10. Williams JC, Richardson R. The continuous mixing of segregating particles. *Powder Technol*. 1982;33(1):5–16.
11. Nauman EB. Residence time theory. *Ind Eng Chem Res*. 2008;47(10):3752–3766.
12. Yeh A-I, Jaw Y-M. Modeling residence time distributions for single screw extrusion process. *J Food Eng*. 1998;35(2):211–232.
13. Ziegler GR, Aguilar CA. Residence time distribution in a co-rotating, twin-screw continuous mixer by the step change method. *J Food Eng*. 2003;59(2–3):161–167.
14. Abouzeid AZMA, Mika TS, Sastry KV, Fuerstenau DW. The influence of operating variables on the residence time distribution for material transport in a continuous rotary drum. *Powder Technol*. 1974;10(6):273–288.
15. Abouzeid AZM, Fuerstenau DW, Sastry KV. Transport behavior of particulate solids in rotary drums: scale-up of residence time distribution using the axial dispersion model. *Powder Technol*. 1980; 27(2):241–250.
16. Sudah OS, Chester AW, Kowalski JA, Beeckman JW, Muzzio FJ. Quantitative characterization of mixing processes in rotary calciners. *Powder Technol*. 2002;126(2):166–173.
17. Sherritt RG, Chaouki J, Mehrotra AK, Behie LA. Axial dispersion in the three-dimensional mixing of particles in a rotating drum reactor. *Chem Eng Sci*. 2003;58(2):401–415.
18. Berthiaux H, Marikh K, Mizonov V, Ponomarev D, Barantzeva E. Modeling Continuous Powder Mixing by Means of the Theory of Markov Chains. *Part Sci Technol*. 2004;22(4):379–389.
19. Portillo P, Muzzio F, Ierapetritou M. Using compartment modeling to investigate mixing behavior of a continuous mixer. *J Pharma Innovation*. 2008;3(3):161–174.
20. Weineköter R, Reh L. Continuous mixing of fine particles. *Part Part Syst Char*. 1995;12(1):46–53.
21. Shin SH, Fan LT. Characterization of solids mixtures by the discrete fourier transform. *Powder Technol*. 1978;19(2):137–146.
22. Risken H. *The Fokker-Planck Equation: Methods of Solution and Applications*. 2nd ed. Springer; 1996.
23. Zwietering TN. The degree of mixing in continuous flow systems. *Chem Eng Sci*. 1959;11(1):1–15.

Appendix: Continuous Formula of Fourier Series Analysis

Suppose the feed rate $C_{in}(t)$ on the interval $t \in [0, T_{in}]$ is injected into a continuous mixer characterized by the residence time distribution $E(t)$. Due to the second assumption in this study, $E(t)$ is assumed negligible on $t \in (T_{in}, \infty)$. Feed rate and RTD signals are converted onto a new time scale $x \in [-\pi, \pi]$ in order to obtain the standard formula of Fourier series

$$f_{in}(x) = C_{in}(t) \tag{A1}$$

$$e(x) = \frac{T_{in}}{2\pi} E(t) \tag{A2}$$

where $x = 2\pi t/T_{in} - \pi$ is the converted time, while $f_{in}(x)$ and $e(x)$ are the corresponding input and RTD after the conversion. The coefficient $T_{in}/2\pi$ in Eq. A2 guarantees constant

flow rate in different time scales, but in Eq. A1 the value of $f_{in}(x)$ is kept the same as when the time unit of the flow rate is not converted. Due to Eqs. 6 and 7, expressions of $f_{in}(x)$ and $e(x)$ in Fourier series are shown as follow

$$f_{\text{in}}(x) = \frac{a_0}{2} + \sum_{n=1}^{\infty} [a_n \cos(nx) + b_n \sin(nx)], \quad x \in [-\pi, \pi] \quad \text{(A3)}$$

$$a_n = \frac{1}{\pi} \int_{-\pi}^{\pi} f_{\text{in}}(x) \cos(nx) dx; \; b_n = \frac{1}{\pi} \int_{-\pi}^{\pi} f_{\text{in}}(x) \sin(nx) dx \quad \text{(A4)}$$

$$e(x) = \frac{A_0}{2} + \sum_{n=1}^{\infty} [A_n \cos(nx) + B_n \sin(nx)], \quad x \in [-\pi, \pi] \quad \text{(A5)}$$

$$A_n = \frac{1}{\pi} \int_{-\pi}^{\pi} e(x) \cos(nx) dx; \quad B_n = \frac{1}{\pi} \int_{-\pi}^{\pi} e(x) \sin(nx) dx \quad \text{(A6)}$$

In Eqs. A3 and A4, input flow is composed of the average $\overline{f_{in}(x)} = a_0/2$ and the fluctuation components from different frequencies. Applying Eq. 8, the sum of square of these components leads to the overall variance

$$\sigma_{\text{in}}^2 = \frac{\int_{-\pi}^{\pi} (f_{\text{in}}(x) - \overline{f_{\text{in}}(x)})^2 dx}{2\pi} = \sum_{n=1}^{\infty} \frac{a_n^2 + b_n^2}{2} = \sum_{n=1}^{\infty} \frac{s_n^2}{2} \quad \text{(A7)}$$

where $s_n^2/2$ is the contribution from the frequency $f_n = n/T_{in}$ to the output variance. Note that this variance shares the same formula as the variance before time scale conversion. It indicates that if a similar form is obtained in the output variance formula, the filtering ability of the mixer can be defined by comparing the corresponding frequency components of input and output fluctuation signals. Substitute the second assumption into Eq. 9, in which $e(x)$ is negligible on $x \in [\pi, \infty]$:

$$f_{\text{out}}(x) = \int_{-\pi}^{\infty} f_{\text{in}}(x - \theta) e(\theta) d\theta = \int_{-\pi}^{\pi} f_{\text{in}}(x - \theta) e(\theta) d\theta \quad \text{(A8)}$$

where f_{out} (x) is the output flows in the converted time scale. Replace $f_{out}(x)$ by its Fourier series formula in Eq. A3

$$f_{\text{out}}(x) = \frac{a_0}{2} + \int_{-\pi}^{\pi} \sum_{n=1}^{\infty} [a_n \cos n(x - \theta) + b_n \sin n(x - \theta)] e(\theta) d\theta \quad \text{(A9)}$$

In Eq. A9 the mean value of f_{out} (x) is the same as that of $f_{in}(x)$ in Eq. A3. Continue the process of deduction on the right side of Eq. A9 by using Eq. A5

$$\int_{-\pi}^{\pi} \cos n(x - \theta) e(\theta) d\theta = \pi A_n \cos nx + \pi B_n \sin nx \quad \text{(A10)}$$

Similarly

$$\int_{-\pi}^{\pi} \sin n(x - \theta) e(\theta) d\theta = -\pi B_n \cos nx + \pi A_n \sin nx \quad \text{(A11)}$$

Combine Eqs. A9–A11

$$f_{\text{out}}(x) = \frac{a_0}{2} + \sum_{n=1}^{\infty} [\pi(a_n A_n - b_n B_n) \cos nx + \pi(a_n B_n + b_n A_n) \sin nx] \quad \text{(A12)}$$

In Eq. A12, the output flow is composed of the average concentration $\overline{f_{out}(x)} = a_0/2$, and the fluctuation part that is represented by series of sine and cosine functions. The output variance and variance reduction ratio thus can be easily derived from Eq. A12 with similar formula of Eq. A7

$$\begin{aligned} \sigma_{out}^2 &= \pi^2 \sum_{n=1}^{\infty} \frac{(a_n A_n - b_n B_n)^2 + (a_n B_n + b_n A_n)^2}{2} \\ &= \pi^2 \sum_{n=1}^{\infty} \frac{(a_n^2 + b_n^2)(A_n^2 + B_n^2)}{2} \end{aligned} \quad \text{(A13)}$$

$$\frac{1}{VRR} = \frac{\sigma_{\text{out}}^2}{\sigma_{\text{in}}^2} = \frac{\sum_{n=1}^{\infty} (a_n^2 + b_n^2)(A_n^2 + B_n^2)\pi^2}{\sum_{n=1}^{\infty} (a_n^2 + b_n^2)} = \frac{\sum_{n=1}^{\infty} s_n^2 F_n^2 \pi^2}{\sum_{n=1}^{\infty} s_n^2} \quad \text{(A14)}$$

In Eq. A14 $F_n^2 \pi^2$ represents the filtering effect of the continuous mixer on the frequency $n\Delta f = n/T_{\text{in}}$. In this formula of variance reduction ratio, axial flow variances (fluid part of VRR in Eq. 5) are clearly decomposed into series of components contributed from different frequencies. This makes it possible to estimate the feeder effect on the performance of the mixer in a theoretical prospective.

Manuscript received Nov. 6, 2009, and revision received May 24, 2010.